Behavioral/Systems/Cognitive

A Discrete GABAergic Relay Mediates Medial Prefrontal Cortical Inhibition of the Neuroendocrine Stress Response

Jason J. Radley,[1] Kristin L. Gosselink,[2] and Paul E. Sawchenko[1]

[1]Laboratory of Neuronal Structure and Function, The Salk Institute for Biological Studies and Clayton Medical Research Foundation, La Jolla, California 92037, and [2]Department of Biological Sciences, University of Texas at El Paso, El Paso, Texas 79968

Complementing its roles in cognitive and affective information processing, the medial prefrontal cortex (mPFC) is a nodal point of a limbic forebrain circuit that modulates stress-related homeostatic mechanisms, including the hypothalamic–pituitary–adrenal (HPA) axis. mPFC influences on HPA output are predominantly inhibitory and emanate from the prelimbic and/or dorsal anterior cingulate cortical fields (PL and ACd, respectively). mPFC projections do not target HPA effector neurons in the paraventricular hypothalamic nucleus (PVH) directly, distributing instead to nearby forebrain regions, including some that house GABAergic neurons implicated in inhibitory PVH control. To identify pathway(s) subserving HPA-inhibitory mPFC influences, an initial screen for sources of GABAergic input to PVH whose sensitivity to an acute emotional (restraint) stress was diminished by PL/ACd lesions identified a discrete region of the anterior bed nucleus of the stria terminalis (aBST) as a candidate for fulfilling this role. Anatomical tracing experiments confirmed projections from PL (but not ACd) to implicated aBST cell groups, and from these to PVH. Finally, selective immunotoxin-mediated ablation of GABAergic aBST neurons recapitulated the effects of PL/ACd lesions on acute stress-induced activation of HPA output. The identification of a proximate mediator of HPA-inhibitory limbic influences provides a framework for clarifying how inhibitory neural and hormonal controls of HPA output are integrated, adaptations of the axis to chronic stress are effected, and how endocrine abnormalities may contribute to stress-related psychiatric illnesses in which mPFC dysfunction is implicated.

Introduction

Inhibitory mechanisms play important roles in limiting adverse catabolic and immunosuppressive effects of engaging the neuroendocrine (hypothalamic–pituitary–adrenal; HPA) stress response, particularly under conditions of repeated or prolonged stress exposure. Both neural (neurons using the inhibitory neurotransmitter GABA) and hormonal (glucocorticoid negative feedback) mechanisms are implicated in the negative regulation of the HPA axis (Sapolsky et al., 1984; Kovács and Makara, 1988; Herman et al., 2003). Cell groups in the limbic forebrain that are enriched in glucocorticoid receptor expression (Diorio et al., 1993; Akana et al., 2001) are activated in a stereotyped manner in response to acute emotional stress (Cullinan et al., 1995; Li and Sawchenko, 1998), and lesion studies have identified several of these as participating in the inhibitory control of neurosecretory neurons in the paraventricular hypothalamic nucleus (PVH) that express corticotropin-releasing factor (CRF) for the initiation of HPA axis responses to stress (Sapolsky et al., 1984; Diorio et al., 1993; Herman et al., 1995). Prominent among these is the medial prefrontal cortex (mPFC), which is involved in the modulation of attentional states and in regulating cognitive and emotional information processing (Whalen et al., 1998; Bush et al., 2000). These attributes are critical for comparing present with past experiences, and assigning valence to emotionally salient stimuli. Congruent with this, the mPFC also actively regulates neuroendocrine and autonomic responses to stress (Neafsey, 1990; Diorio et al., 1993; Radley et al., 2006a). mPFC impairment is associated with cognitive and affective symptoms of stress-related psychiatric illnesses (Shin et al., 2007; Liberzon and Sripada, 2008), to which HPA axis dysregulation may contribute in a feedforward manner.

None of the limbic cell groups implicated in negative HPA regulation, including mPFC, provide any substantial direct innervation of the PVH, leading to the widely held view that their stress-inhibitory influences are imparted via interposed GABAergic neurons (Herman et al., 2003). The fact that such GABAergic cell groups have not yet been identified has left open a host of issues as to how the corticosteroid-dependent and -independent inhibitory controls of the axis are organized and integrated. The present study sought to define this circuitry for the mPFC.

An initial experiment aimed to localize identified GABAergic PVH-afferent cell groups whose engagement following acute emotional stress exposure was diminished by ablation of dorsal mPFC, implicated previously in HPA inhibition. This pointed to contiguous components of the anterior bed nucleus of the stria terminalis (aBST), notably the fusiform (BSTfu) and dorsomedial (BSTdm) subdivisions of Swanson and colleagues (Ju and

Received Dec. 12, 2008; revised April 9, 2009; accepted April 30, 2009.

This work was supported by National Institutes of Health Grant DK-26741 and was conducted in part by the Clayton Medical Research Foundation. P.E.S. is an Investigator of the Clayton Medical Research Foundation. J.J.R. is supported by a National Alliance for Research on Schizophrenia and Depression Young Investigator award. We thank J. Vaughn for generating the Fos antiserum and Drs. J. Serrats and R. Rissman for antiserum characterization. We also thank Casey Peto for help in imaging, Kris Trulock for help in the preparation of the illustrations, Linda Feighery and Belle Wamsley for editorial assistance, Carlos Arias and Marty Mortrud for technical assistance, and Yaira Haas for assistance with radioimmunoassay.

Correspondence should be addressed to Dr. Jason J. Radley, Laboratory of Neuronal Structure and Function, The Salk Institute, 10010 North Torrey Pines Road, La Jolla, CA 92037. E-mail: radley@salk.edu.

DOI:10.1523/JNEUROSCI.5924-08.2009

 0270-6474/09/297330-11$15.00/0

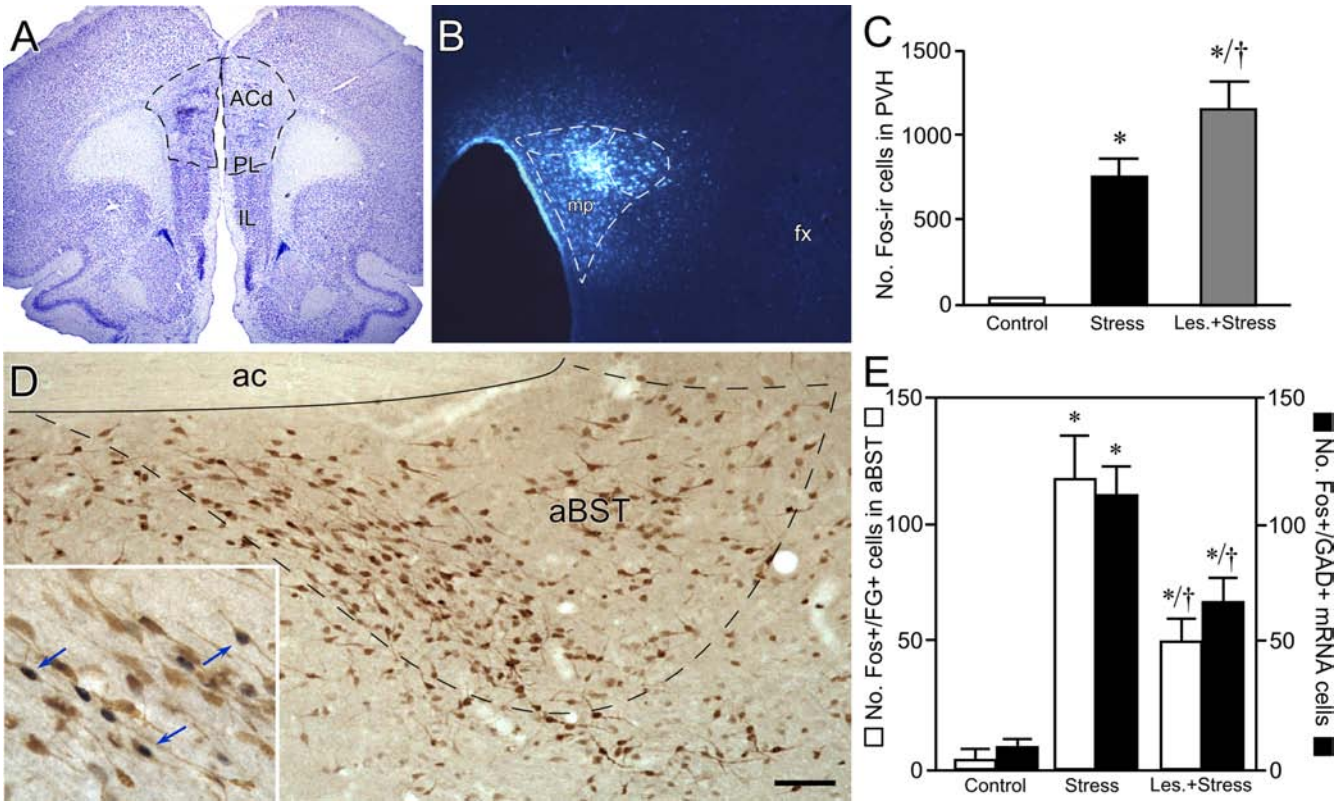

Figure 1. Activational responses of PVH-projecting GABAergic cell groups in aBST following acute restraint are diminished by excitotoxin lesions to dorsal mPFC. ***A***, Nissl preparation of a coronal section from representative dorsal mPFC-lesioned animal. Damage from excitotoxin lesions was centered in PL, with spread into ACd. IL, Infralimbic area. ***B***, Photomicrograph showing a Fluoro-Gold tracer deposit in PVH. Tracer injections were centered in PVH and involved the medial parvicellular (mp) part of the PVH, which houses hypophysiotropic neurons that govern HPA output. fx, Fornix. ***C***, Histogram showing effects of dorsal mPFC lesions on restraint-induced cellular activation in PVH. Mean + SEM number of Fos-immunoreactive (-ir) neurons in PVH is shown; lesioned animals displayed the expected enhancement of stress-induced activational responses. ***D***, Bright-field photomicrograph showing stress-induced Fos-immunoreactive (black nuclei) and Fluoro-Gold (brown cytoplasm) in aBST. Retrogradely labeled cells are concentrated in fusiform and dorsomedial subdivisions of aBST. The inset shows examples (arrows) of cells doubly labeled for Fos and Fluoro-Gold at higher magnification. ac, Anterior commissure. ***E***, Mean + SEM number of neurons colabeled for Fos and Fluoro-Gold (open bars), and for Fos and GAD67 mRNA (black bars) in aBST in treatment groups. Lesions reliably diminished stress-induced activation of PVH-projecting and GABAergic neurons in aBST. $^{*}p < 0.05$, differs significantly from unstressed controls; $^{\dagger}p < 0.05$, differs significantly from sham-lesioned stress animals. $n = 4–5$ per group. Scale bar (in ***D***): ***A***, 1 mm; ***B***, 300 μm; ***D***, 100 μm; inset, 50 μm.

Swanson, 1989; Dong et al., 2001; Dong and Swanson, 2006), as candidate mediators of mPFC influences on the stress axis. Complementary tract tracing experiments confirmed prelimbic area (PL) projections to BSTfu/dm (but not PVH, proper), and prominent aBST inputs to PVH (Dong et al., 2001; Dong and Swanson, 2006). Finally, the hypothesized functional involvement of an aBST relay in modulating stress-induced HPA activation was tested by the focal administration of an immunotoxin, anti-GABA-transporter-1-saporin (antiGAT-1-sap), which preferentially ablates GABAergic neurons expressing GAT-1. The results support a PL→BSTfu/dm (GABAergic)→PVH pathway effecting mPFC inhibition of HPA responses to acute emotional stress.

Materials and Methods

Animals and treatments. Adult male Sprague Dawley albino rats, maintained under standard laboratory conditions, were used in all experiments. All experimental protocols were approved by the Institutional Animal Care and Use Committee of the Salk Institute. Restraint stress was performed in the morning (9:00 A.M.) in plastic restrainers (Braintree Scientific) for 30 min. Controls were handled comparably, but were not restrained. All animals remained in their home cages during and after restraint until the prescribed time of perfusion for histology (2 h after the termination of restraint), or during collection of repeated blood samples.

Surgeries. Axon-sparing excitotoxin lesions were produced via bilateral pressure ejection of ibotenic acid (10 mg/ml, Sigma) in sterile saline centered in PL, as previously described (Radley et al., 2006a). To selectively ablate GABAergic neurons in BSTfu/dm, antiGAT-1-sap (conjugates of saporin with a rabbit polyclonal antiserum raised against a peptide in the extracellular domain of the GABA transporter-1; Advanced Targeting Systems) were microinjected either unilaterally or bilaterally. A stock solution (1.9 mg/ml) was diluted 1:2 in artificial CSF (aCSF) at pH 7.4. Injections were placed via micropipettes (10–20 μm, inner diameter) using pressure ejection (World Precision Instruments) to deliver 120 nl per side at the following stereotaxic coordinates: anteroposterior (AP) = −0.25 mm; mediolateral (ML) = ±1.20 mm; dorsoventral (DV) = −7.20 mm (from dura). Control lesions involved either injecting saporin conjugated to IgG, or the aCSF vehicle. The extent and specificity of damage was estimated by reconstruction from material hybridized for the 67 kDa isoform of the GABA-synthetic enzyme, glutamic acid decarboxylase (GAD67), and CRF mRNA.

For retrograde labeling of PVH-projecting neurons, iontophoretic injections (+5 μA, 7 s on/off) of 2% Fluoro-Gold (Fluorochrome) (Schmued and Fallon, 1986) were made into PVH (AP = −1.4; ML = +0.4; DV = −7.4). Anterograde tracing experiments involved the following: (1) pressure ejection of 10% biotinylated dextran amine (BDA) (Sigma) made into PL (AP = +2.90; ML = +0.75; DV = −2.5); (2) unilateral iontophoretic injection (+5 μA, 7 s on/off) of 2.5% PHA-L (Vector Laboratories) centered in BSTfu. Both anterograde tracers provide high-resolution labeling of axons and terminals. Iontophoretic deposition of PHA-L yields very discrete injection sites (Gerfen and Sawchenko, 1984), which was considered optimal for targeting circumscribed subregions of the bed nucleus. The size of BDA deposits delivered

by pressure ejection varies directly with injection volume, and this allowed more effective sampling of the much larger PL cortical field.

Histology and tissue processing. Rats were anesthetized with chloral hydrate (350 mg/kg, i.p.) and perfused via the ascending aorta with 100 ml of 0.9% saline followed by 900 ml of ice-cold 4% paraformaldehyde in 0.1 M borate buffer, pH 9.5, at a flow rate of 55 ml/min. The brains were removed, postfixed for 3 h, and cryoprotected in 20% sucrose in 0.1 M phosphate buffer overnight at 4°C. Five one-in-five series of 30-μm-thick frozen coronal sections through the entire brain were cut and collected in cryoprotectant solution and stored at −20°C until processing.

Histochemistry. Localization of Fos protein and other antigens were performed by using an avidin-biotin peroxidase protocol (Sawchenko et al., 1990) to localize a primary antiserum raised against a fragment of rat Fos protein (residues 4–17), generously synthesized by J. Rivier (Salk Institute) and previously characterized (Radley et al., 2008). Dual immunoperoxidase labeling for Fos and Fluoro-Gold immunoreactivity was performed by sequentially localizing the antiserum against Fos using a nickel-enhanced diaminobenzidine method (black nuclear reaction product) (Shu et al., 1988), as above, and then a Fluoro-Gold antiserum (Chang et al., 1990), without nickel enhancement (brown cytoplasmic product). Specificity of the Fos antiserum was evaluated by direct colabeling for *c-fos* mRNA over a range of challenge conditions (data not shown). In addition, specific staining in experimental and control tissue was abolished by preadsorbing the antiserum overnight at 4°C with 50 μM of the synthetic peptide immunogen.

Techniques for probe synthesis, hybridization, and autoradiographic localization of mRNA signal were adapted from Simmons et al. (1989). *In situ* hybridization was performed using ^{35}S-labeled sense (control) and antisense cRNA probes labeled to similar specific activities using a full-length probe for mRNA encoding CRF (1.2 kb; Dr. K. Mayo, Northwestern University, Evanston, IL), and the 67 kDa isoform of glutamic acid decarboxylase (GAD67, Dr. A. Tobin, University of California, Los Angeles, Los Angeles, CA) (Erlander et al., 1991). Probes for the vesicular glutamate transporter, types 1 and 2 (VGLUT1 and VGLUT2) were derived from mouse cDNAs (Open Biosystems) bearing a high degree of homology to rat (VGLUT1: 96% homology to nucleotides 65–437 of rat VGLUT1, GenBank accession number BE950784; Dr. H. Chin, National Institute of Mental Health, Bethesda, MD; VGLUT2: 94% homology to nucleotides 545–1070 of rat VGLUT2, accession number CB247147; Dr. R. Strausberg, National Institutes of Health, Bethesda, MD). Hybridization using antisense probes for VGLUT1 and VGLUT2 yielded labeling that conformed with the reported distributions in rat brain (Ziegler et al., 2002), and sense probes for each did not provide evidence of specific labeling. A GAT-1 probe (Dr. H. J. Lester, California Institute of Technology, Pasadena, CA) was derived from a cDNA encompassing the entire open reading frame of mouse GAT-1 (Chiu et al., 2002), and supported a localization pattern similar to that described in rat brain (Durkin et al., 1995). Combined immunoperoxidase and isotopic hybridization histochemical localization of Fos immunoreactivity and GAD67 mRNA, respectively, was performed using a modification of protocols detailed previously (Chan et al., 1993).

Hormone assays. Separate groups of animals were implanted with indwelling jugular catheters 12 d after receiving bilateral immunotoxin or sham lesions in BSTfu/dm, and 2 d before stress exposure. The procedures for implanting catheters have been described previously (Ericsson et al., 1994). Blood samples (300 μl) were taken before restraint stress to estimate basal ACTH and corticosterone levels. Additional samples were collected at 0, 30, 60, and 90 min after the termination of restraint. ACTH was measured using a two-site immunoradiometric assay obtained in kit form (DiaSorin), with intra-assay and interassay coefficients of variation of 3 and 9%, respectively, and a sensitivity of 1.5 pg/ml. Plasma corticosterone was measured without extraction, using an antiserum raised in rabbits against a corticosterone-BSA conjugate, and ^{125}I-corticosterone-BSA as tracer (MP Biomedicals). The sensitivity of the assay was 0.8 μg/dl; intra-assay and interassay coefficients of variation were 5 and 10%, respectively.

Table 1. Effect of mPFCd lesions on functional activation in PVH-projecting cell groups following acute restraint stress

	No. Fos-labeled nuclei		No. Fos + FG-labeled cells	
PVH-projecting cell groups	Sham	mPFCd lesion	Sham	mPFCd lesion
Vicinity of PVH				
Anterior hypothalamic area	310 ± 40	368 ± 68	23 ± 8	28 ± 1
Anterior PVH	234 ± 42	254 ± 24	37 ± 14	32 ± 12
Perisupraoptic area	365 ± 20	467 ± 47	63 ± 8	34 ± 19
Perifornical area	479 ± 112	534 ± 31	54 ± 29	72 ± 14
Zona incerta	325 ± 10	478 ± 28*	33 ± 13	38 ± 3
Other regions				
aBST	285 ± 55	377 ± 99	125 ± 23	53 ± 10*
Dorsomedial hypothalamus	645 ± 113	543 ± 59	120 ± 8	79 ± 10*
Medial preoptic area	425 ± 31	484 ± 120	44 ± 11	60 ± 20

Values represent mean ± SEM for counts made within each region. Statistical comparisons were made using a one-way ANOVA (control, sham + stress, lesion + stress), followed by *post hoc* pairwise comparisons using a Bonferroni correction (data from unstressed controls are not shown). Asterisk indicates significance ($p < 0.05$).

Data analysis. Stereological methods were used to quantify the number of Fos-immunoreactive neurons. These analyses were performed using a computer-assisted morphometry system consisting of a photomicroscope equipped with an *X–Y–Z* computer-controlled motorized stage, MicroFire camera (Optronics), Gateway microcomputer, and StereoInvestigator morphometry and stereology software (MBF Biosciences). For each analysis, boundaries defining the regions of interest were drawn at 25× using an adjacent series of Nissl-stained sections. In regions identified as PVH-projecting (i.e., retrogradely labeled following FG injections in PVH), labeled cells were used as a guide to further aid the delineation of anatomical boundaries. Analyses of Fos-immunoreactive cells were performed on every fifth section, avoiding cells in the outermost plane of focus. Counts were then multiplied by five to estimate the total number of labeled neurons in the defined region of interest. Volume estimates from cross-sectional area measurements were obtained using the Cavalieri method to probe for possible treatment effects on PVH volume, but no reliable effects were observed. FG- and GAD-labeled neurons (and those doubly labeled for Fos protein) were counted manually in every fifth section (experiment 1). In these analyses, the section thickness was too small relative to the average diameter of labeled neurons in order to permit stereologic approaches, and estimates of cell numbers were obtained using the Abercrombie correction (Abercrombie, 1949).

Semiquantitative densitometric analysis of relative levels of GAD67 and CRF mRNA were performed on emulsion-coated slides using ImageJ software. The optical densities of hybridization signals were determined under dark-field illumination at 100× magnification. The hypophysiotropic PVH (i.e., dorsal medial parvicellular subdivision) was defined from Nissl staining pattern (Swanson and Kuypers, 1980) and aligned with corresponding dark-field images of hybridized sections by redirected sampling. The anterior BST was defined from a combination of Nissl staining and axonal fiber tracts (Dong et al., 2001). Optical density readings, corrected for background, were taken at regularly, 150 μm intervals and average values were determined through the extent of this cell group for each animal. Images from GAD67 and CRF mRNA densitometry were collected using a Hamamatsu Orca CCD camera under the control of OpenLab software (version 3.1.5). Images collected from each analysis were exported first to Adobe Photoshop (version 7) for adjustments to optimize/balance contrast and brightness, and then to Canvas (version 8) for assembly and labeling.

Statistics. Grouped data from the immunoperoxidase and hybridization histochemical analyses ($n = 4$–5 per group) were compared with a one-way ANOVA for lesion and treatment (sham + control, sham + stress, lesion + stress) status followed by *post hoc* pairwise comparisons using a Bonferroni correction. Group data from the hormone assays ($n = 5$ per group) were compared with a mixed-design ANOVA with one within-

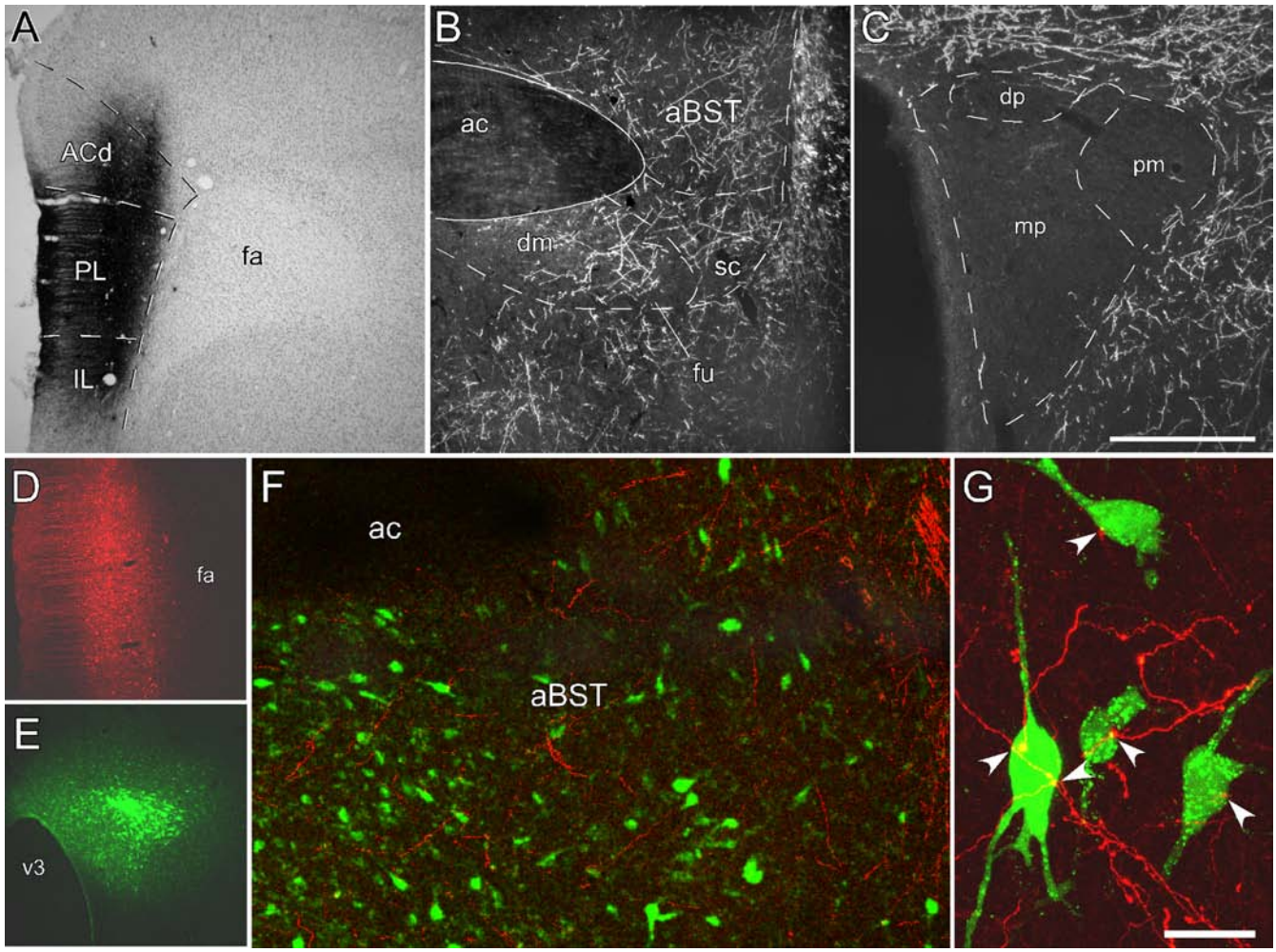

Figure 2. Anterograde tracing studies support PL influences on PVH, via BSTfu/dm. ***A***, Bright-field photomicrograph showing a large-bearing deposit of the anterograde tracer, BDA, centered in PL. ***B***, ***C***, Dark-field photomicrographs showing anterogradely labeled fibers and terminals in aBST (***B***) and the PVH region (***C***), following BDA injection in PL. ***D–G***, Confocal images of dual immunofluorescence preparations show overlap between PL inputs and PVH-projecting neurons in aBST. Animals receiving BDA injections in PL (red, ***D***) and Fluoro-Gold injections in PVH (green, ***E***) show an overlap of axonal labeling (red) in aBST and neurons (green) that project to PVH (***F***). fa, Forceps anterior of the corpus callosum; v3, third ventricle. ***G***, A digital reconstruction of dual fluorescence labeling of BDA and Fluoro-Gold in BSTfu/dm is shown, that was acquired using a 63× oil objective (NA 1.4) with a zoom of 2×, in 0.75 μm *z*-steps throughout the entire extent of the 30-μm-thick section. Arrows point to examples where terminals were found to be in close apposition with retrogradely labeled elements, derived from examination of single optical planes containing fluorescence labeling for both markers. Scale bars: (in ***C***) ***A***, 1 mm; ***B***, ***C***, 500 μm; (in ***G***) ***D***, ***E***, 300 μm; ***F***, 100 μm; ***G***, 10 μm.

(time) and one between- (lesion status) group variable, followed by individual pairwise comparisons as above. Data are expressed as the mean ± SEM.

Results

Effects of dorsal mPFC lesions on stress-induced activation of PVH-projecting cell groups

We previously localized inhibitory influences of mPFC over PVH/HPA responses to acute emotional stress to the dorsal mPFC, including the PL and dorsal anterior cingulate area (ACd) (Radley et al., 2006a, 2008). These areas project weakly, if at all, to the PVH proper, distributing instead to nearby regions of the basal forebrain and hypothalamus (Sesack et al., 1989; Hurley et al., 1991), including some that house GABAergic neurons that could mediate inhibitory control imparted from mPFC (Cullinan et al., 1993; Roland and Sawchenko, 1993). An initial experiment sought to identify GABAergic cell groups that might subserve this role. To this end, excitotoxin lesions were placed in dorsal mPFC, a retrograde tracer (Fluoro-Gold) was injected into PVH, and we assayed PVH-afferent cell groups for lesion-induced reductions in sensitivity to acute restraint (Fig. 1*A*,*B*). Dual immunostaining was performed for Fluoro-Gold and Fos protein expression, a generic marker of neuronal activation, in sham-lesioned unstressed controls, and in sham- and dorsal mPFC-lesioned animals 2 h after the termination of restraint stress. We verified our previous observations that cellular activational responses (Fos) in PVH are reliably increased following 30 min of restraint stress, and are further enhanced (by 41%) following dorsal mPFC lesions, relative to sham-lesioned controls ($p < 0.05$) (Fig. 1*C*). Alterations in Fos activation in PVH have been found to be predictive of changes in pituitary–adrenal secretory responses under these conditions (Radley et al., 2006a).

In sham-lesioned rats subjected to restraint, six distinct regions of the hypothalamus, including the preoptic area, anterior hypothalamic area, perifornical area, perisupraoptic area, dorsomedial (DMH) and ventromedial hypothalamic nuclei, and several subdivisions of aBST displayed colocalization of Fos and transported tracer, thus representing stress-sensitive PVH afferents (Table 1). Of these, only DMH and contiguous components of aBST, the BSTfu and BSTdm nuclei, exhibited reliable decrements (35% and 54%, respectively) in the number of cells labeled concurrently for Fos and tracer in acutely stressed rats bearing

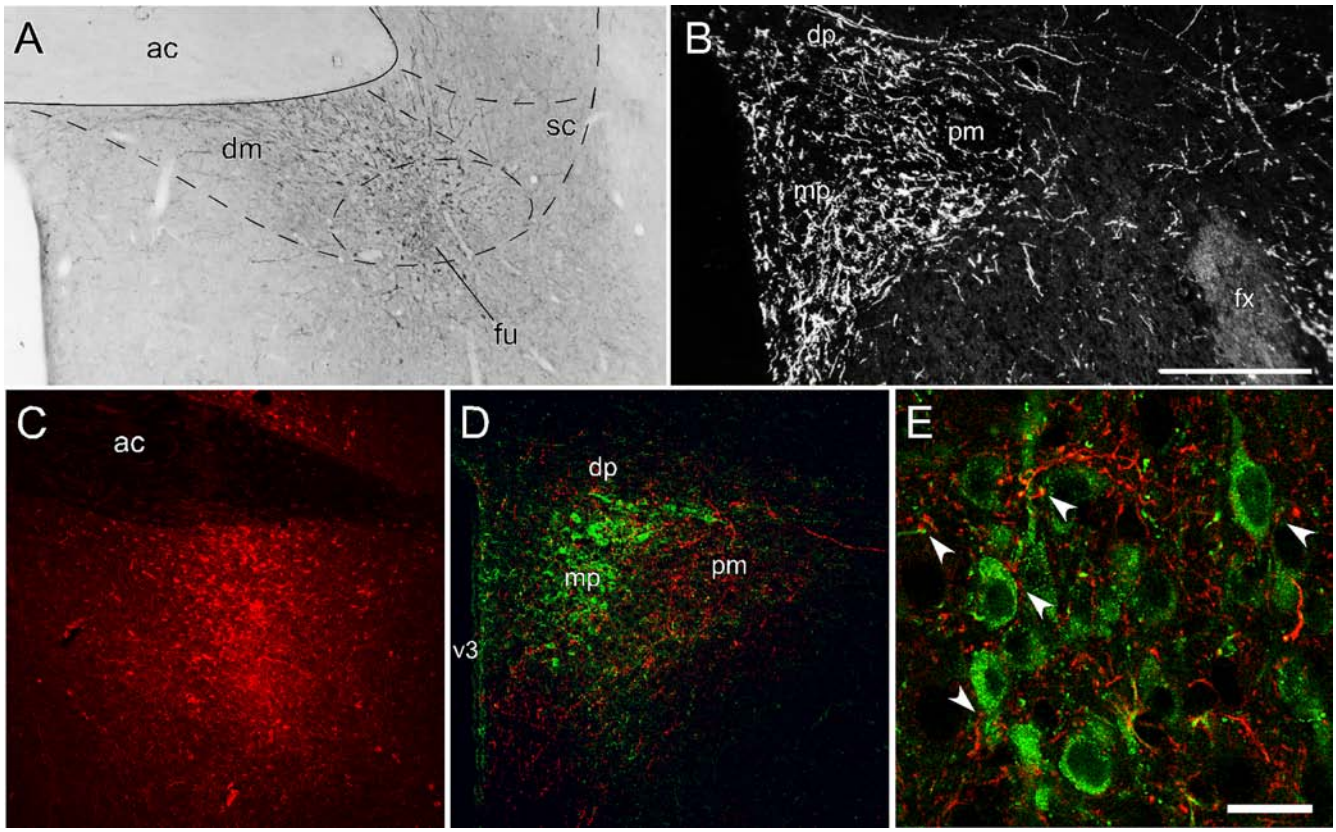

Figure 3. ***A***, Bright-field photomicrograph showing immunoperoxidase staining of a small deposit of the anterograde tracer, PHA-L, centered in the fusiform subdivision (fu) of aBST. ***B***, Dark-field image of PHA-L-labeled axon fibers and terminals in PVH following discrete injections centered in BSTfu. dm, Dorsomedial nucleus (aBST); dp, dorsal parvicellular part (PVH); mp, medial parvicellular part (PVH); pm, posterior magnocellular part (PVH); sc, subcommissural nucleus (aBST). ***C–E***, Confocal images of dual fluorescence preparations showing extensive overlap and appositions between anterogradely labeled terminal fields (red) and neurons immunoreactive for CRF (green) in PVH. Animals received BDA injections centered in the fusiform and dorsomedial subdivisions of aBST (***C***) and were adrenalectomized to upregulate CRF expression in stress-related neurosecretory neurons in PVH (***D***). In ***E***, arrowheads indicate examples of BDA-labeled terminals in close apposition to CRF-labeled perikarya or dendrites in a single optical section (63× oil objective, NA 1.4, zoom of 2×). Scale bars: (in ***B***) ***A***, ***B***, 250 μm; (in ***E***) ***C***, 250 μm; ***D***, 100 μm; ***E***, 10 μm.

dorsal mPFC lesions compared with sham-lesioned animals ($p < 0.05$ for each region). Subsequent analyses in aBST and DMH involving combined histochemical localization of Fos protein and mRNA encoding the 67 kDa isoform of glutamate decarboxylase (GAD67; a marker of GABAergic neurons) revealed a significant decrement only in aBST (by 58%; $p < 0.05$) (Fig. 1*D*,*E*). This occurred despite the lack of a lesion effect on overall stress-induced Fos expression in aBST, and the lack of between-group differences in the number of retrogradely labeled cells in this region (supplemental Fig. 1, available at www.jneurosci.org as supplemental material).

Anterograde tracing experiments support aBST as a potential relay between PL and PVH

To determine whether implicated aspects of the aBST receive mPFC input, and thus represent candidate mediators of HPA-inhibitory prefrontal influences, complementary anterograde tracing experiments were performed involving pressure injections of BDA, into different mPFC subfields. Histochemical visualization of transported BDA revealed multiple descending pathways from mPFC. mPFC projections reach the BST by diverging medially at the level of the anterior commissure from fiber bundles coursing through the internal capsule to invade the anterodorsal, anteroventral, and anteromedial divisions of BST. The density of axonal/terminal innervation of aBST varied topographically in a dorsal-to-ventral manner. BDA injections centered in ACd ($n = 4$), the most dorsal aspect of mPFC, failed to label projections to aBST. More ventrally placed deposits labeled progressively more substantial inputs to BSTfu/dm, with deposits restricted to PL ($n = 4$) giving rise to an overall moderate innervation (Fig. 2*A*,*B*). Coupled with evidence from lesion studies (Diorio et al., 1993; Figueiredo et al., 2003; Radley et al., 2006a), these findings implicate PL, but not ACd, in the inhibition of stress-induced activation of PVH. It is noteworthy that large deposits of BDA into PL labeled few, if any, projections invading the medial parvicellular part of the PVH, which houses CRF-expressing neurons that govern HPA output (Fig. 2*C*). Separate experiments in which rats ($n = 5$) received BDA injections in PL and Fluoro-Gold injections centered in PVH, revealed PL projections that ramify extensively among PVH-projecting neurons in BSTfu/dm, with frequent juxtaposition of anterogradely labeled varicosities with retrogradely filled perikarya or dendrites (Fig. 2*D*–*G*).

A second set of tracing experiments using the anterogradely transported plant lectin *Phaseolus vulgaris*-leucoagglutinin (PHA-L) was performed to confirm (Dong et al., 2001; Dong and Swanson, 2006) that implicated aspects of the aBST project to the PVH. PHA-L injections centered in several aBST subregions ($n = 4$) produced robust labeling of axonal fibers and terminals throughout the anterior hypothalamus and in regions closely adjoining the PVH, with moderate terminal innervation throughout PVH proper, inclusive of both its magnocellular and parvicellular divisions. However, PHA-L injections centered in BSTdm and/or BSTfu ($n = 4$) labeled very prominent inputs to

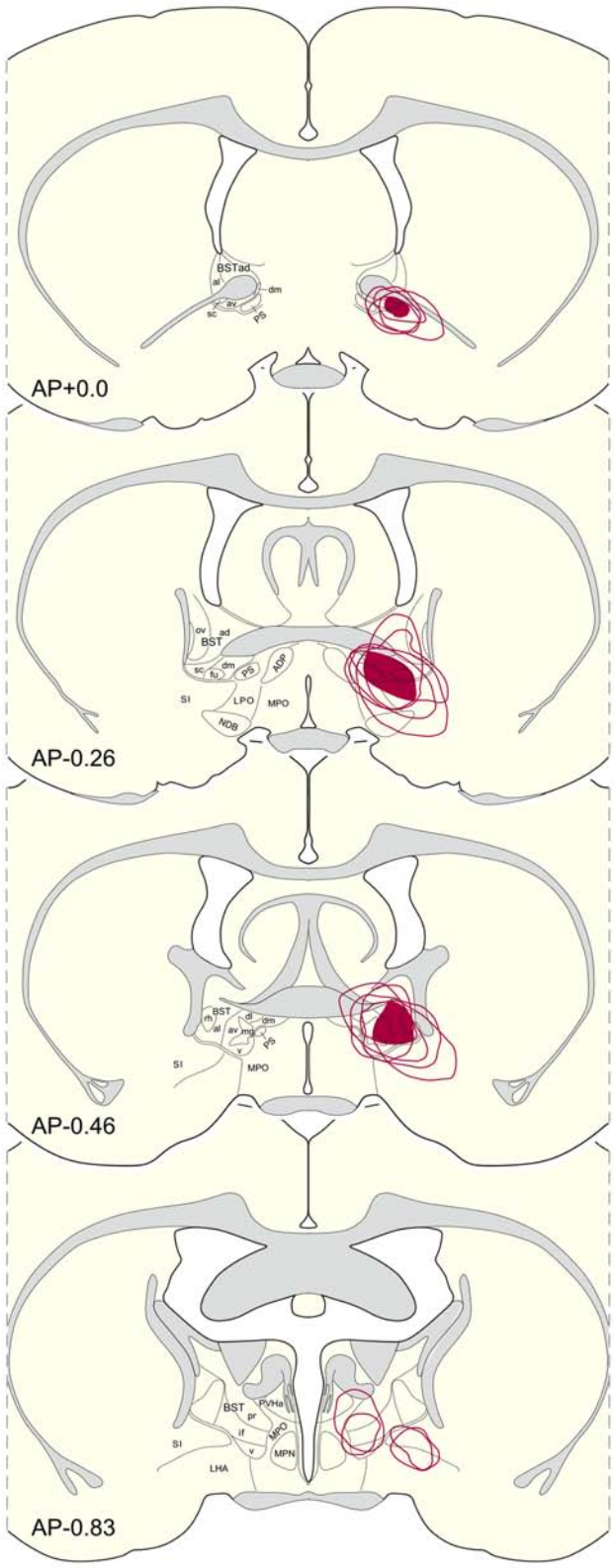

Figure 4. Reconstruction of antiGAT-1-sap lesion placements. Solid areas of red represent the region of damage common to all members of each group and outlines the extent of individual lesions, as defined by depletion of GAD67 mRNA-expressing cells. GABAergic cell loss was most pronounced in BSTfu/dm and with variable involvement of other adjoining cell groups (anteroventral and anterolateral subdivisions, av and al, respectively; and rhomboid nucleus, rh). Atlas plates are based on Swanson (1992); their distance in millimeters relative to bregma is indicated. ADP, Anterodorsal preoptic nucleus; BST subdivisions: ad, anterodorsal area; dl, dorsolateral nucleus; dm, dorsomedial nucleus; fu, fusiform nucleus; if, interfascicular nucleus; mg, magnocellular nucleus; ov, oval nucleus; pr, principal nucleus; sc, subcommissural nucleus; v, ventral nucleus; LHA, lateral hypothalamic area; LPO, lateral preoptic area; MPN, medial preoptic nucleus; MPO, medial preoptic area; NDB, nucleus of the diagonal band; PS, parastrial nucleus; PVHa, paraventricular hypothalamic nucleus, anterior part; SI, substantia innominata.

the PVH whose terminal ramifications included the hypophysiotropic zone, with minimal labeling of the magnocellular division and PVH-surround regions (Fig. 3*A*, *B*). In separate experiments, anterograde tracing from the aBST was performed in rats ($n = 5$) that were adrenalectomized, to upregulate CRF expression in stress-related neurosecretory neurons of the PVH. Confocal microscopic analysis of this material revealed frequent close appositions between labeled axonal elements and CRF-expressing parvicellular neurons (Fig. 3*C–E*).

Effects of unilateral ablation of GABAergic cells in aBST on PVH activational responses to acute restraint

While the foregoing data are consistent with the thesis that PL influences over stress-induced PVH/HPA activation are conveyed via a disynaptic inhibitory pathway involving GABAergic cell groups in BSTfu/dm, functional evidence to support this hypothesis is lacking. We sought to provide this by using a GABA neuron immunotoxin (antiserum to the GABA transporter, GAT-1, coupled to the ribosomal toxin, saporin; antiGAT-1-sap) to assess the effect of disrupting GABAergic elements in aBST on indices of basal and stress-induced HPA activation. GAT-1 is the most widely distributed GAT in rat brain, and is abundant in basal forebrain (Durkin et al., 1995). Preliminary experiments ($n = 3$) confirmed robust expression of GAT-1 in the aBST, including in identified PVH-projecting cells (supplemental Fig. 2, available at www.jneurosci.org as supplemental material). Since the initial experiments implicate the dorsomedial, and in particular, fusiform subdivisions of BST in relaying inhibitory influences of PL over stress-induced indices of PVH activation, immunotoxin injections were centered in these regions. The extent of unilateral immunotoxin lesions was evaluated by hybridization histochemical localization of GAD67. Representative immunotoxin lesions to aBST are shown in Figure 4. Selective targeting of inhibitory cell groups was facilitated by initial tests of the immunotoxin at varying concentrations, and assessing the extent of both GAD67 mRNA depletion and nonspecific damage, i.e., to different phenotypic markers (CRF, substance P, VGLUT1 and VGLUT2 mRNAs). The areas of damage common to all cases included, anterior aspects of the subcommissural, anteroventral, dorsomedial, and fusiform nuclei of the BST, portions of the parastrial nucleus, and at their caudalmost extent, portions of the rhomboid and anterolateral parts of the BST. Specificity of antiGAT-1-sap was evaluated by comparison of multiple mRNA transcripts indicative of distinct neuronal phenotypes within the BSTfu/dm in separate series of sections throughout the injection site. First, GAD67 and VGLUT mRNA were examined in adjacent series to evaluate the effect of the antiGAT-1-sap on inhibitory and excitatory neuron subpopulations in BSTfu/dm. The BSTfu/dm showed an abundance of GAD67-expressing cells on the sham-lesioned (intact) side, and were virtually absent on the injected side (Fig. 5). While VGLUT expression was relatively low in the aBST, no frank differences were evident in VGLUT1 and/or VGLUT2 mRNAs as assessed both densitometrically and by cell counts in BSTfu/dm on the lesioned, relative to the intact sides ($p = 0.8$) (supplemental Fig. 3, available at www.jneurosci.org as supplemental material).

Further characterization of immunotoxin specificity in-

←

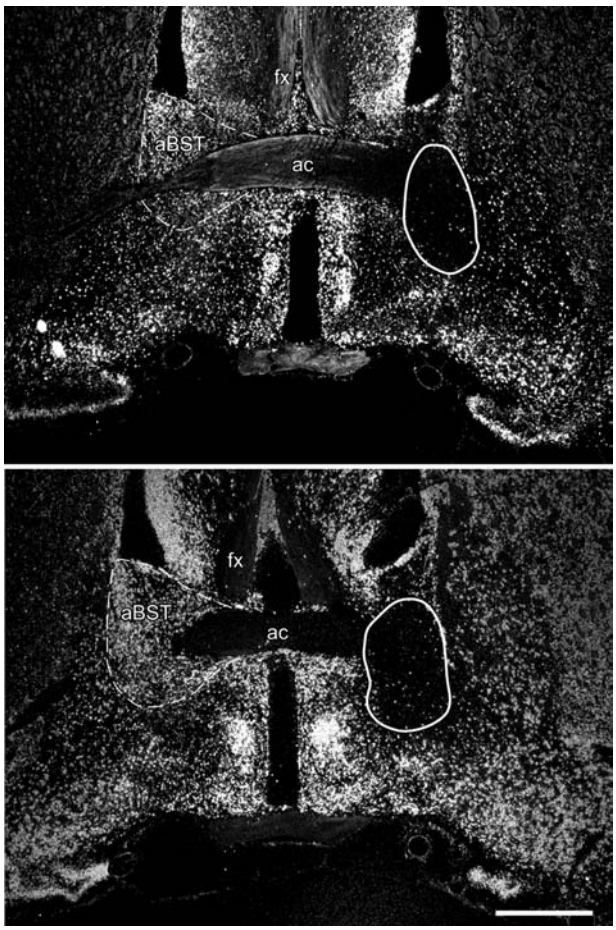

Figure 5. Immunotoxin-mediated depletion of GABAergic neurons in the aBST region. Low-magnification dark-field photomicrographs from a representative experiment showing GAD67 mRNA expression at two levels of the aBST, on the sides ipsilateral (right) and contralateral (left) to a unilateral antiGAT-1-sap injection. The approximate extent of GABAergic cell loss is outlined. Scale bar, 1 mm (applies to both).

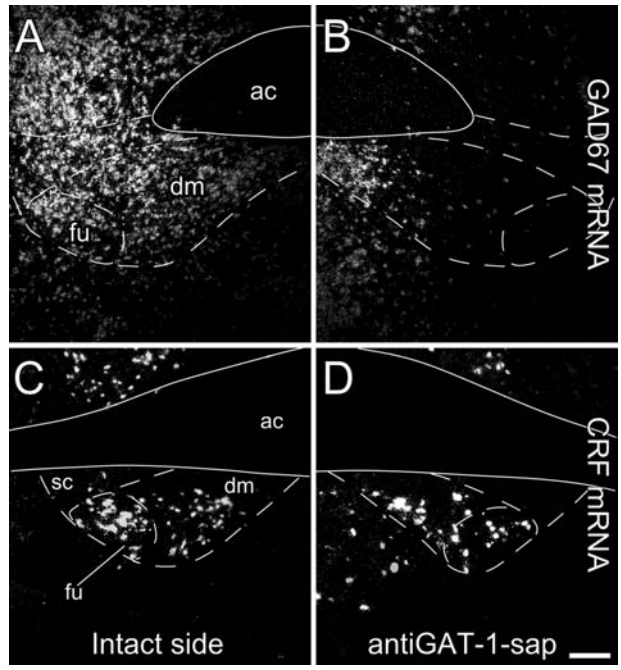

Figure 6. Unilateral antiGAT-1-sap lesions centered in BSTfu/dm preferentially ablate GABAergic neurons. Top, Dark-field photomicrographs showing GAD67 mRNA expression in aBST on the intact (***A***) and lesioned (immunotoxin-injected; ***B***) sides of the brain, showing that a large population of neurons in BSTfu/dm subdivisions are GABAergic, and vulnerable to depletion by local antiGAT-1-sap injection. Bottom, Dark-field photomicrographs of CRF mRNA expression in an adjacent section from the same animal, illustrating that numerous cell groups in BSTdm, and particularly BSTfu, also express CRF mRNA (***C***). These populations are largely spared following immunotoxin injections (***D***). Scale bar, 125 μm (applies to all).

volved the analysis of CRF mRNA expression in another series of sections and comparison with GAD67 mRNA distribution (Fig. 6). This was also of functional interest, in view of evidence to support an excitatory influence of CRF-expressing cells in BSTfu/dm on HPA activity (Choi et al., 2007). CRF-expressing cells were moderately dense in BSTfu, and less so in the BSTdm on the intact side (Fig. 6*C*). Immunotoxin lesions to aBST resulted in a minimal loss of CRF-expressing cells in these subnuclei (Fig. 6*D*), supporting a preferential targeting of GABAergic neurons. Densitometric analyses revealed a significant decrease (by 80%, $p < 0.01$) in relative levels of GAD67 mRNA in BST fu/dm following immunotoxin lesions, but no reliable effect on CRF mRNA ($p = 0.3$).

Assessments were made of two indices of cellular activation in PVH following 30 min of restraint in animals bearing appropriately placed unilateral immunotoxin lesions of aBST. Whereas the number of cells expressing Fos protein in PVH were elevated following 30 min of restraint compared with unstressed controls regardless of lesion status ($p < 0.05$), measures of both Fos protein (Fig. 7*A*,*B*) and CRF mRNA (Fig. 7*C*,*D*) expression displayed significantly greater enhancements following 30 min of acute restraint (by 77% and 52%, respectively) on the side of PVH ipsilateral to the immunotoxin injection in aBST, compared with the intact side ($p < 0.05$ for each) (Fig. 7*E*).

Effects of ablating GABAergic cells in aBST on stress-induced hormone secretion

HPA secretory responses before and after 30 min restraint stress were examined in separate groups of sham and bilaterally immunotoxin-lesioned animals. Despite differences in mean peak ACTH levels between groups, data from the sham-lesioned animals were variable, and these did not differ significantly. Nonetheless, within-group comparisons revealed that in bilateral immunotoxin-lesioned animals, plasma ACTH remained significantly elevated above prestress levels for a longer duration, compared with sham-lesioned animals (at 60 min: $p < 0.05$ and $p = 0.3$, respectively) (Fig. 8*A*). Plasma corticosterone levels showed reliable main effects of lesion ($p = 0.01$) (Fig. 8*B*), with bilateral immunotoxin lesioned animals showing a 67% enhancement of plasma corticosterone values at the peak (30 min) time point compared with sham-lesioned animals ($p < 0.05$). Basal plasma levels of ACTH and corticosterone were not affected by the lesions ($p = 0.6$ and 0.2, respectively), suggesting that the effects of ablating GABAergic neurons in aBST are manifest during stress.

Discussion

In an initial study, acute restraint-induced cellular activation of PVH was exaggerated following excitotoxin lesions of dorsal mPFC, verifying involvement of this cortical region in HPA inhibition during emotional stress exposure (Diorio et al., 1993; Figueiredo et al., 2003; Radley et al., 2006a). Inferences drawn from comparison of regional dual labeling patterns in separate series of sections, suggested that acute restraint-induced activation of PVH-projecting GABAergic cell groups in BSTfu/dm was

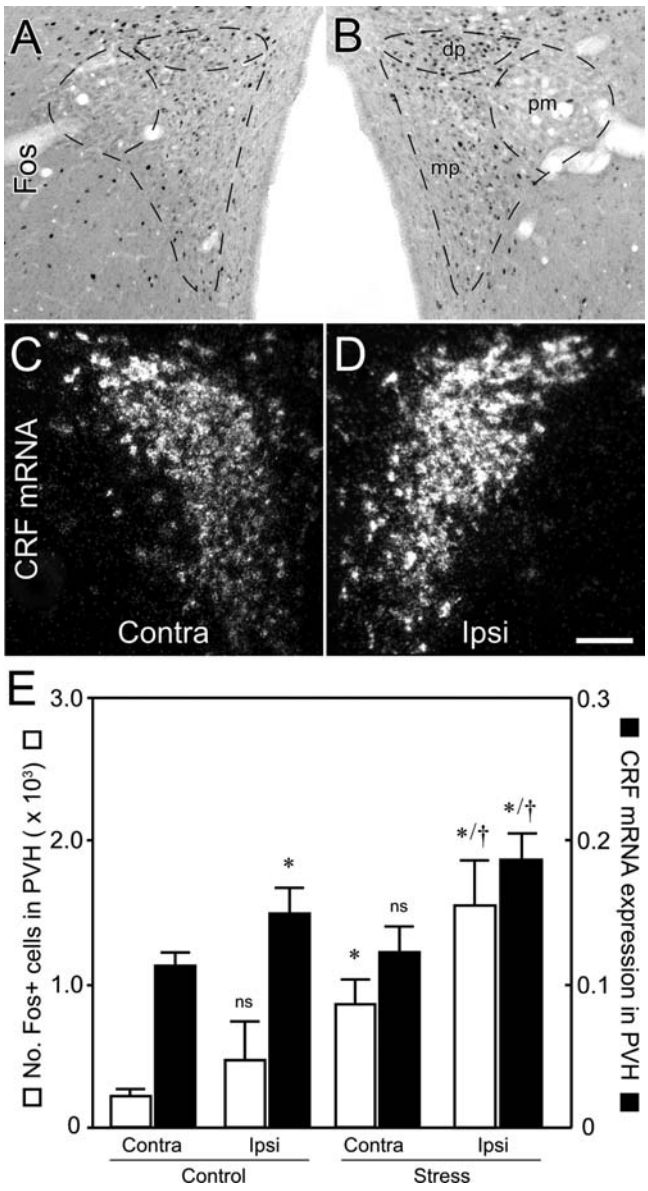

Figure 7. Unilateral immunotoxin injections centered in BSTfu/dm enhance restraint-induced indices of HPA activation. Bright- (***A***, ***B***) and dark- (***C***, ***D***) field photomicrographs illustrate that restraint-induced upregulation of both Fos immunoreactivity and CRF mRNA expression is enhanced in the PVH on the side ipsilateral (Ipsi) to immunotoxin lesions of aBST, relative to the intact (Contra) side of the brain. ***E***, Mean + SEM number of Fos-immunoreactive neurons (open bars) and relative levels of CRF mRNA (black bars) in PVH in all treatment groups. $*p <$ 0.05, differs significantly from the contralateral PVH of unstressed controls; $^{\dagger}p < 0.05$, differs significantly from the contralateral PVH of stressed rats; ns, nonsignificant. $n = 5$ per group. Scale bar, 125 μm (applies to all).

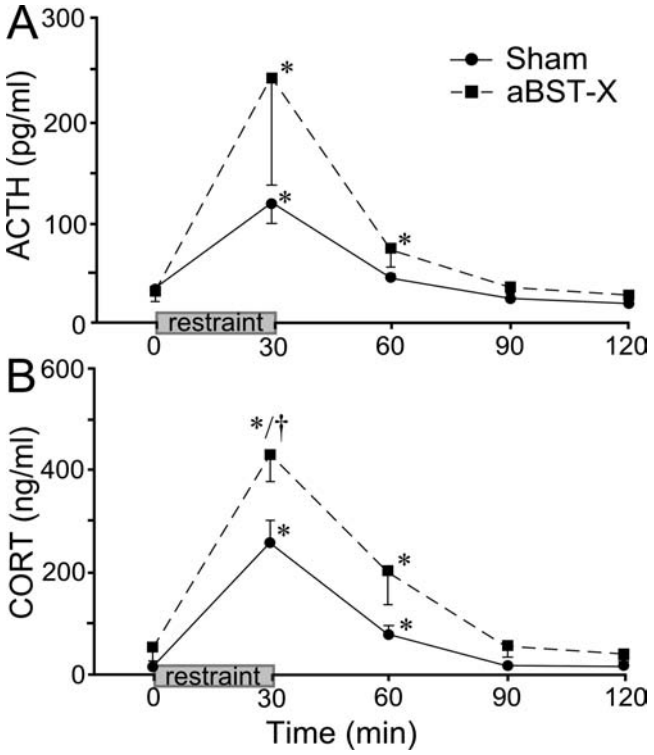

Figure 8. Mean ± SEM plasma ACTH (***A***) and corticosterone (***B***) levels in sham and immunotoxin-injected animals before (0 min) and at varying intervals after acute restraint exposure. Stress significantly increased plasma levels of both hormones in both sham- and bilaterally immunotoxin-lesioned animals. Although plasma ACTH values did not differ reliably at any poststress time point, immunotoxin lesions resulted in a more prolonged increase ($p <$ 0.05 at 30 and 60 min compared with 0 min) and 67% greater peak levels of plasma corticosterone. $*p < 0.05$, differs significantly from basal (0 min) values within each group; $^{\dagger}p < 0.05$, differs significantly from sham-lesioned animals. $n = 5$ per group.

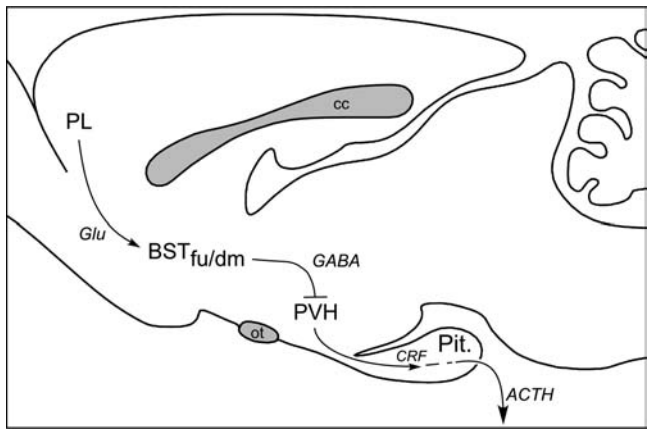

Figure 9. Circuitry providing for mPFCd-inhibitory influences on HPA output. During emotional stress, GABAergic neurons in BSTfu/dm impart restraining influences of mPFC on CRF-expressing neurosecretory neurons that control HPA output. It remains to be determined whether stress-inhibitory influences of other limbic forebrain cell groups are mediated via similar or distinct circuitries. Not illustrated here is evidence for an excitatory projection to PVH from a similar region of the BST (Spencer et al., 2005; Choi et al., 2007).

markedly diminished following excitotoxin lesions of dorsal mPFC. Tracing experiments confirmed that projections of PL, which minimally innervate PVH proper, provide a moderate input to BSTfu/dm, which in turn, densely innervates the CRF-rich neurosecretory zone of the PVH (Fig. 9). The provision of an interposed inhibitory relay from PL to PVH is consistent with evidence that extrinsic mPFC projections are overwhelmingly glutamatergic (Ottersen et al., 1995). In the final experiment, targeted ablation of inhibitory cell groups in BSTfu/dm resulted in the enhancement of multiple indices of PVH and HPA activation in response to restraint stress, closely recapitulating the effects of excitotoxin lesions of PL reported here and previously (Radley et al., 2006a).

This is the first published report endorsing antiGAT-1-sap as a tool for focally ablating GABAergic cell groups in the CNS. GAT-1 is the most widely distributed of the plasma membrane-associated GABA transporters (Durkin et al., 1995; Borden,

1996), and histochemical analyses of cellular GAT-1 expression support its predominant localization to GABAergic neurons, although expression in some regions is limited to subsets of GABAergic cells (Durkin et al., 1995; Borden, 1996). The immunotoxin comprises an antiserum raised against an extracellular GAT-1 sequence to foster targeted internalization of the ribosome-inactivating protein, saporin, to which it is coupled. GAT-1 protein localizes principally to axons and terminals, consistent with predominantly presynaptic sites of action (Borden, 1996), leaving open questions as to the mechanism of immunotoxin targeting and how generally applicable this tool may be. GABAergic neuron loss was apparent only within the area of aBST to which the immunotoxin was focally administered, whereas no frank effects were seen in GABAergic cell groups known to project to aBST (data not shown), notably the lateral part of the central nucleus of the amygdala (Petrovich and Swanson, 1997; Day et al., 1999). This would indicate that the immunotoxin is not effective in lesioning at a distance on the basis of retrograde transport. As our preliminary work indicated that the efficacy and specificity of immunotoxin effects were concentration-dependent, similar groundwork and controls for specificity will be required to employ the method effectively in other systems.

In the present studies, immunotoxin efficacy was indicated by marked decrements in expression of an enzyme marker for GABAergic neurons (GAD67 mRNA), while selectivity was supported by the failure of the toxin to significantly impact mRNA markers of glutamatergic (VGLUT1 and VGLUT2) and peptidergic (substance P, CRF) neurons. The BSTfu neurons display a similar complement of neurochemical phenotypes as the more dorsally situated oval nucleus of the BST complex, including GABA and CRF (Ju and Swanson, 1989; Day et al., 1999; Dong et al., 2001). Although CRF and GABA are coexpressed in a substantial subpopulation of oval nucleus neurons (Day et al., 1999; Dong et al., 2001), our data suggest that these phenotypes are largely distinct in BSTfu/dm. Furthermore, the possibility remains that the tendency toward reduction of the CRF complement following immunotoxin injection, although not statistically reliable, could be indicative of a small subset of BSTfu neurons that coexpress GAD and CRF.

A focus on the BSTfu/dm was mandated by results of initial experiments implicating these cell groups as sources of GABAergic input to PVH whose sensitivity to acute emotional stress was diminished by dorsal mPFC lesions. Preferential ablation of GABAergic cell groups in BSTfu/dm enhanced central and hormonal indices of stress-induced HPA output in a manner that closely recapitulated the effects of excitotoxin lesions of dorsal mPFC on acute restraint-induced HPA output (Radley et al., 2006a). An inhibitory role for BSTfu/dm was unanticipated in light of recent studies reporting attenuation of HPA responses to acute restraint following indiscriminate excitotoxin lesions to aBST (Spencer et al., 2005; Choi et al., 2007), from which it was concluded that CRF-expressing cell groups in BSTfu/dm exert a stimulatory influence on stress-induced HPA activation (Choi et al., 2007). The present finding of an effect opposite in sign following ablations that target GABAergic neurons preferentially while sparing CRF-expressing ones is consonant with this interpretation. Other studies have shown that stimulation of the aBST can facilitate or inhibit HPA activity (Dunn, 1987; Casada and Dafny, 1991), supporting the idea of distinct HPA-regulatory influences arising from neurochemically differentiated BST subpopulations.

The identification of a relatively discrete cell cluster that is necessary and sufficient for the exertion of stress-inhibitory mPFC influences should provide a framework for addressing lingering organizational issues in central HPA control. First, other stress-sensitive limbic forebrain cell regions, notably the hippocampal formation and septal region, have been implicated in HPA inhibition (McEwen et al., 1968; Dobrakovová et al., 1982), and it is unclear if these effects are mediated independently, or may share a common arbiter in the aBST. There already exists strong evidence that this general region of the BST mediates influences of the ventral subiculum (Cullinan et al., 1993). It is also noteworthy that implicated regions of the aBST receive prominent inputs from the central nucleus of the amygdala, among other cell groups involved in central autonomic control (Dong et al., 2001; Dong and Swanson, 2006), likely defining an additional layer of integration of stress-related effector mechanisms. Second, and related, is the fact that these same limbic structures, including mPFC, comprise candidate sites of corticosteroid negative feedback regulation of HPA output (Diorio et al., 1993; Sánchez et al., 2000; Akana et al., 2001). Knowledge of an inhibitory relay of mPFC influences, at least, will facilitate designing experiments to parse steroid-dependent and -independent components of limbic control. Third, adaptations such as habituation or facilitation are important determinants of adverse health consequences of repeated stress exposure, yet there remain gaps in understanding the neural substrates of these phenomena. Either can be eliminated by lesioning a midline thalamic cell group, the posterior paraventricular thalamic nucleus (PVTp) (Bhatnagar and Dallman, 1998; Bhatnagar et al., 2002), but the proximate mediators of PVTp influences are unclear. In this light, it is of interest that the PVTp issues a moderate projection to BSTfu/dm (Li and Kirouac, 2008), while not targeting the PVH at all, and innervating preferentially the ventral (infralimbic) part of mPFC (Berendse and Groenewegen, 1991).

PFC dysfunction is implicated in a range of psychiatric disorders that may be precipitated (e.g., posttraumatic stress disorder) or exacerbated (forms of depression) by stress (Hains and Arnsten, 2008). These conditions are associated with disordered HPA regulation (Mason et al., 1986; Plotsky et al., 1998), which is apt to contribute to pathology, as repeated emotional stress exposure in animal models gives rise to regressive alterations in mPFC morphology and function (Radley et al., 2006b; Cerqueira et al., 2007; Liu and Aghajanian, 2008). In defining a proximate link between the mPFC and HPA control, the present findings allow assessment of the effects of perturbing key stress-modulatory pathways on affective disease mechanisms, with the promise of highlighting novel targets for pharmacotherapeutic intervention.

References

Abercrombie M (1949) Estimation of nuclear populations from microtome populations sections. Anat Rec 94:239–247.

Akana SF, Chu A, Soriano L, Dallman MF (2001) Corticosterone exerts site-specific and state-dependent effects in prefrontal cortex and amygdala on regulation of adrenocorticotropic hormone, insulin and fat depots. J Neuroendocrinol 13:625–637.

Berendse HW, Groenewegen HJ (1991) Restricted cortical termination fields of the midline and intralaminar thalamic nuclei in the rat. Neuroscience 42:73–102.

Bhatnagar S, Dallman M (1998) Neuroanatomical basis for facilitation of hypothalamic-pituitary-adrenal responses to a novel stressor after chronic stress. Neuroscience 84:1025–1039.

Bhatnagar S, Huber R, Nowak N, Trotter P (2002) Lesions of the posterior paraventricular thalamus block habituation of hypothalamic-pituitary-adrenal responses to repeated restraint. J Neuroendocrinol 14:403–410.

Borden LA (1996) GABA transporter heterogeneity: pharmacology and cellular localization. Neurochem Int 29:335–356.
Bush G, Luu P, Posner MI (2000) Cognitive and emotional influences in anterior cingulate cortex. Trends Cogn Sci 4:215–222.
Casada JH, Dafny N (1991) Restraint and stimulation of bed nucleus of the stria terminalis produce similar stress-like behaviors. Brain Res Bull 27:207–212.
Cerqueira JJ, Mailliet F, Almeida OF, Jay TM, Sousa N (2007) The prefrontal cortex as a key target of the maladaptive response to stress. J Neurosci 27:2781–2787.
Chan RK, Brown ER, Ericsson A, Kovács KJ, Sawchenko PE (1993) A comparison of two immediate-early genes, c-fos and NGFI-B, as markers for functional activation in stress-related neuroendocrine circuitry. J Neurosci 13:5126–5138.
Chang HT, Kuo H, Whittaker JA, Cooper NG (1990) Light and electron microscopic analysis of projection neurons retrogradely labeled with Fluoro-Gold: notes on the application of antibodies to Fluoro-Gold. J Neurosci Methods 35:31–37.
Chiu CS, Jensen K, Sokolova I, Wang D, Li M, Deshpande P, Davidson N, Mody I, Quick MW, Quake SR, Lester HA (2002) Number, density, and surface/cytoplasmic distribution of GABA transporters at presynaptic structures of knock-in mice carrying GABA transporter subtype 1-green fluorescent protein fusions. J Neurosci 22:10251–10266.
Choi DC, Furay AR, Evanson NK, Ostrander MM, Ulrich-Lai YM, Herman JP (2007) Bed nucleus of the stria terminalis subregions differentially regulate hypothalamic-pituitary-adrenal axis activity: implications for the integration of limbic inputs. J Neurosci 27:2025–2034.
Cullinan WE, Herman JP, Watson SJ (1993) Ventral subicular interaction with the hypothalamic paraventricular nucleus: evidence for a relay in the bed nucleus of the stria terminalis. J Comp Neurol 332:1–20.
Cullinan WE, Herman JP, Battaglia DF, Akil H, Watson SJ (1995) Pattern and time course of immediate early gene expression in rat brain following acute stress. Neuroscience 64:477–505.
Day HE, Curran EJ, Watson SJ Jr, Akil H (1999) Distinct neurochemical populations in the rat central nucleus of the amygdala and bed nucleus of the stria terminalis: evidence for their selective activation by interleukin-1beta. J Comp Neurol 413:113–128.
Diorio D, Viau V, Meaney MJ (1993) The role of the medial prefrontal cortex (cingulate gyrus) in the regulation of hypothalamic-pituitary-adrenal responses to stress. J Neurosci 13:3839–3847.
Dobrakovová M, Kvetnanský R, Torda T, Murgas K (1982) Changes of plasma and adrenal catecholamines and corticosterone in stressed rats with septal lesions. Physiol Behav 29:41–45.
Dong HW, Swanson LW (2006) Projections from bed nuclei of the stria terminalis, dorsomedial nucleus: implications for cerebral hemisphere integration of neuroendocrine, autonomic, and drinking responses. J Comp Neurol 494:75–107.
Dong HW, Petrovich GD, Watts AG, Swanson LW (2001) Basic organization of projections from the oval and fusiform nuclei of the bed nuclei of the stria terminalis in adult rat brain. J Comp Neurol 436:430–455.
Dunn JD (1987) Plasma corticosterone responses to electrical stimulation of the bed nucleus of the stria terminalis. Brain Res 407:327–331.
Durkin MM, Smith KE, Borden LA, Weinshank RL, Branchek TA, Gustafson EL (1995) Localization of messenger RNAs encoding three GABA transporters in rat brain: an in situ hybridization study. Brain Res Mol Brain Res 33:7–21.
Ericsson A, Kovács KJ, Sawchenko PE (1994) A functional anatomical analysis of central pathways subserving the effects of interleukin-1 on stress-related neuroendocrine neurons. J Neurosci 14:897–913.
Erlander MG, Tillakaratne NJ, Feldblum S, Patel N, Tobin AJ (1991) Two genes encode distinct glutamate decarboxylases. Neuron 7:91–100.
Figueiredo HF, Bruestle A, Bodie B, Dolgas CM, Herman JP (2003) The medial prefrontal cortex differentially regulates stress-induced c-fos expression in the forebrain depending on type of stressor. Eur J Neurosci 18:2357–2364.
Gerfen CR, Sawchenko PE (1984) An anterograde neuroanatomical tracing method that shows the detailed morphology of neurons, their axons and terminals: immunohistochemical localization of an axonally transported plant lectin, *Phaseolus vulgaris* leucoagglutinin (PHA-L). Brain Res 290:219–238.
Hains AB, Arnsten AF (2008) Molecular mechanisms of stress-induced prefrontal cortical impairment: implications for mental illness. Learn Mem 15:551–564.
Herman JP, Cullinan WE, Morano MI, Akil H, Watson SJ (1995) Contribution of the ventral subiculum to inhibitory regulation of the hypothalamo-pituitary-adrenocortical axis. J Neuroendocrinol 7:475–482.
Herman JP, Figueiredo H, Mueller NK, Ulrich-Lai Y, Ostrander MM, Choi DC, Cullinan WE (2003) Central mechanisms of stress integration: hierarchical circuitry controlling hypothalamo-pituitary-adrenocortical responsiveness. Front Neuroendocrinol 24:151–180.
Hurley KM, Herbert H, Moga MM, Saper CB (1991) Efferent projections of the infralimbic cortex of the rat. J Comp Neurol 308:249–276.
Ju G, Swanson LW (1989) Studies on the cellular architecture of the bed nuclei of the stria terminalis in the rat: I. Cytoarchitecture. J Comp Neurol 280:587–602.
Kovács KJ, Makara GB (1988) Corticosterone and dexamethasone act at different brain sites to inhibit adrenalectomy-induced adrenocorticotropin hypersecretion. Brain Res 474:205–210.
Li HY, Sawchenko PE (1998) Hypothalamic effector neurons and extended circuitries activated in "neurogenic" stress: a comparison of footshock effects exerted acutely, chronically, and in animals with controlled glucocorticoid levels. J Comp Neurol 393:244–266.
Li S, Kirouac GJ (2008) Projections from the paraventricular nucleus of the thalamus to the forebrain, with special emphasis on the extended amygdala. J Comp Neurol 506:263–287.
Liberzon I, Sripada CS (2008) The functional neuroanatomy of PTSD: a critical review. Prog Brain Res 167:151–169.
Liu RJ, Aghajanian GK (2008) Stress blunts serotonin- and hypocretin-evoked EPSCs in prefrontal cortex: role of corticosterone-mediated apical dendritic atrophy. Proc Natl Acad Sci U S A 105:359–364.
Mason JW, Giller EL, Kosten TR, Ostroff RB, Podd L (1986) Urinary free-cortisol levels in posttraumatic stress disorder patients. J Nerv Ment Dis 174:145–149.
McEwen BS, Weiss JM, Schwartz LS (1968) Selective retention of corticosterone by limbic structures in rat brain. Nature 220:911–912.
Neafsey EJ (1990) Prefrontal cortical control of the autonomic nervous system: anatomical and physiological observations. Prog Brain Res 85:147–165, discussion 165–166.
Ottersen OP, Hjelle OP, Osen KK, Laake JH (1995) Amino acid transmitters, Ed 2. San Diego: Academic.
Petrovich GD, Swanson LW (1997) Projections from the lateral part of the central amygdalar nucleus to the postulated fear conditioning circuit. Brain Res 763:247–254.
Plotsky PM, Owens MJ, Nemeroff CB (1998) Psychoneuroendocrinology of depression. Hypothalamic-pituitary-adrenal axis. Psychiatr Clin North Am 21:293–307.
Radley JJ, Arias CM, Sawchenko PE (2006a) Regional differentiation of the medial prefrontal cortex in regulating adaptive responses to acute emotional stress. J Neurosci 26:12967–12976.
Radley JJ, Rocher AB, Miller M, Janssen WG, Liston C, Hof PR, McEwen BS, Morrison JH (2006b) Repeated stress induces dendritic spine loss in the rat medial prefrontal cortex. Cereb Cortex 16:313–320.
Radley JJ, Williams B, Sawchenko PE (2008) Noradrenergic innervation of the dorsal medial prefrontal cortex modulates hypothalamo-pituitary-adrenal responses to acute emotional stress. J Neurosci 28:5806–5816.
Roland BL, Sawchenko PE (1993) Local origins of some GABAergic projections to the paraventricular and supraoptic nuclei of the hypothalamus in the rat. J Comp Neurol 332:123–143.
Sánchez MM, Young LJ, Plotsky PM, Insel TR (2000) Distribution of corticosteroid receptors in the rhesus brain: relative absence of glucocorticoid receptors in the hippocampal formation. J Neurosci 20:4657–4668.
Sapolsky RM, Krey LC, McEwen BS (1984) Glucocorticoid-sensitive hippocampal neurons are involved in terminating the adrenocortical stress response. Proc Natl Acad Sci U S A 81:6174–6177.
Sawchenko PE, Cunningham ETJ, Mortrud MT, Pfeiffer SW, Gerfen CR (1990) Phaseolus vulgaris-leucoagglutinin (PHA-L) anterograde axonal transport technique. Methods Neurosci 3:247–260.
Schmued LC, Fallon JH (1986) Fluoro-Gold: a new fluorescent retrograde axonal tracer with numerous unique properties. Brain Res 377:147–154.

Sesack SR, Deutch AY, Roth RH, Bunney BS (1989) Topographical organization of the efferent projections of the medial prefrontal cortex in the rat: an anterograde tract-tracing study with Phaseolus vulgaris leucoagglutinin. J Comp Neurol 290:213–242.

Shin LM, Bush G, Whalen PJ, Handwerger K, Cannistraro PA, Wright CI, Martis B, Macklin ML, Lasko NB, Orr SP, Pitman RK, Rauch SL (2007) Dorsal anterior cingulate function in posttraumatic stress disorder. J Trauma Stress 20:701–712.

Shu SY, Ju G, Fan LZ (1988) The glucose oxidase-DAB-nickel method in peroxidase histochemistry of the nervous system. Neurosci Lett 85:169–171.

Simmons DM, Arriza JL, Swanson LW (1989) A complete protocol for in situ hybridization of messenger RNAs in brain and other tissues with radiolabeled single-stranded RNA probes. J Histotechnol 12:169–181.

Spencer SJ, Buller KM, Day TA (2005) Medial prefrontal cortex control of the paraventricular hypothalamic nucleus response to psychological stress: possible role of the bed nucleus of the stria terminalis. J Comp Neurol 481:363–376.

Swanson LW (1992) Brain maps: structure of the rat brain. Amsterdam: Elsevier.

Swanson LW, Kuypers HG (1980) The paraventricular nucleus of the hypothalamus: cytoarchitectonic subdivisions and organization of projections to the pituitary, dorsal vagal complex, and spinal cord as demonstrated by retrograde fluorescence double-labeling methods. J Comp Neurol 194:555–570.

Whalen PJ, Bush G, McNally RJ, Wilhelm S, McInerney SC, Jenike MA, Rauch SL (1998) The emotional counting Stroop paradigm: a functional magnetic resonance imaging probe of the anterior cingulate affective division. Biol Psychiatry 44:1219–1228.

Ziegler DR, Cullinan WE, Herman JP (2002) Distribution of vesicular glutamate transporter in rat hypothalamus. J Comp Neurol 448:217–229.